DE GRUYTER
OPEN

Arch. Min. Sci., Vol. 61 (2016), No 4, p. 823–852

Electronic version (in color) of this paper is available: http://mining.archives.pl

DOI 10.1515/amsc-2016-0056

MASOUD RANJBARNIA*[1], AHMAD FAHIMIFAR**, PIERPAOLO ORESTE***

NEW ANALYTICAL APPROACHES FOR EVALUATING THE PERFORMANCE OF SYSTEMATIC PRE-TENSIONED FULLY GROUTED ROCKBOLTS IN TUNNEL STABILIZATION

NOWE ANALITYCZNE METODY OCENY SKUTECZNOŚCI DZIAŁANIA WSTĘPNIE NAPRĘŻANYCH ZACEMENTOWANYCH KOTEW PRZY STABILIZACJI TUNELI

In this paper, two new analytical approaches are presented on the basis of convergence-confinement method to compute both the ultimate convergence of circular tunnel and its plastic zone having been reinforced by systematically pre-tensioned fully grouted rockbolts. The models have two basic assumptions: (1) the grouted rockbolts increase the radial internal pressure within a broken rock mass by both the pre-tensioned force and the probable following induced force due to rock mass movement (2) tunnel convergence (specially short-term) occurs only due to reducing and diminishing of the radial constrained stress on tunnel surface provided by the working face. Hence, the values of both the pre-tensioned pressure and the mentioned radial constrained stress are specially taken into consideration in this paper. That is, according to their magnitudes, two different conditions occur: the magnitude of pre-tensioned pressure is greater than that of the constrained stress at bolt installation time and vice versa. The solutions are extended to each of conditions, and illustrative examples are solved. The proposed approaches predicting almost identical results show that pre-tensioning of grouted rockbolts will increase the efficiency and effectiveness of rockbolts.

Keywords: analytical approach; tunneling design; convergence-confinement method; pre-tensioned fully grouted rockbolt

W pracy tej przedstawiono dwie analityczne metody oparte na metodzie badania konwergencji i naprężeń wymuszonych wykorzystane do obliczania zarówno granicznej konwergencji tunelu o przekroju koła oraz zachowania strefy plastycznej, po wzmocnieniu tunelu za pomocą wstępnie naprężanych i zacementowanych kotew. Model opiera się dwóch założeniach: (1) zacementowane kotwy prowadzą do wzrostu ciśnienia wewnętrznego w kierunku promieniowym w kruszonym materiale skalnym, spowodowanego siłą wstępnego naprężenia oraz siłą spowodowaną przez ruchy górotworu; (2) – konwergencja

* UNIVERSITY OF TABRIZ, FACULTY OF CIVIL ENGINEERING, DEPARTMENT OF GEOTECHNICAL ENGINEERING, EAST AZERBAIJAN, TABRIZ, 29 BAHMAN BLVD, IRAN. E-mail: m.ranjbarnia@tabrizu.ac.ir

** AMIRKABIR UNIVERSITY OF TECHNOLOGY (TEHRAN POLYTECHNIC), FACULTY OF CIVIL AND ENVIRONMENTAL ENGINEERING, DEPARTMENT OF GEOTECHNICAL ENGINEERING, TEHRAN, HAFEZ AVE, IRAN. E-mail: fahim@aut.ac.ir

*** POLITECNICO DI TORINO, FACULTY OF ENVIRONMENTAL, LAND AND INFRASTRUCTURE ENGINEERING, TURIN, CORSO DUCA DEGLI ABRUZZI, 24, 10129, ITALY. E-mail: pierpaolo.oreste@polito.it

[1] CORRESPONDING AUTHOR: E-mail: m.ranjbarnia@tabrizu.ac.ir

tunelu (zwłaszcza w ujęciu krótkoterminowym) pojawia się jedynie wskutek zmniejszenia wymuszonego naprężenia promieniowego na powierzchni tunelu generowanego w rejonie przodka wydobywczego. W metodzie zwrócono szczególną uwagę na wartości ciśnienia wstępnego naprężenia jak i naprężenia wymuszonego. W zależności od wielkości tych naprężeń mamy do czynienia z dwiema zupełnie odmiennym sytuacjami: wielkość ciśnienia wstępnego naprężenia jest większa niż naprężenia wymuszonego w trakcie mocowania kotew, lub odwrotnie. Podano rozwiązania dla obydwu rozważanych przypadków i zaprezentowano przykłady. Prawie identyczne wyniki otrzymane przy użyciu obydwu metod wskazują, że wstępne naprężenia cementowanych kotew poprawia ich skuteczność działania.

Słowa kluczowe: metody analityczne, projektowanie tuneli, metoda obliczania konwergencji i naprężeń wymuszonych, wstępnie naprężane zacementowane kotwy

1. Introduction

The use of systematic grouted rockbolts as a standard practice in design and construction of tunnels is widely increased due to their effectiveness e.g. in new technologies such as New Austrian Tunnelling Method (NATM) and their other advantageous e.g. speed, minimum installation space and cost. This stabilizing system can be installed as either passive or active (pre-tensioned) types which the aim of pre-tensioning is to transfer initial compressive pressure to rock mass in order to increase its performance and its efficiency (Carranza-Torres, 2009).

The study of behavior mechanism of grouted rockbolts as the systematic reinforcing support has been of considerable interest during the last three decades. A number of analytical methods of varying degrees of accuracy, efficiency, and sophistication have been developed. Among these works, in a group of approaches, it has been attempted to obtain the engineering properties of reinforced rock mass as an improved composite material (Ranjbarnia et al., 2014a, 2015). However, in another group of approaches, the grouted bolt have been considered as an individual element which its contribution to rock mass is in the form of a radial load inducing the radial pressure within the influence domain of itself (Ranjbarnia et al., 2014a, 2015).

In the first group, which the engineering properties of rock mass is assumed to be improved due to bolting effect, Indraratna and Kaiser (1990a, b) introduced a dimensionless parameter named "bolt density" which reflected the relative density of bolts with respect to the opening perimeter to obtain the reinforced rock mass properties. Osgoui and Oreste (2007, 2010) improved Indraratna and Kaiser's solution (1990a, b) by applying "bolt density" parameter into all strength parameters of generalized Hoek-Brown criterion. Bobet (2006) obtained the elastic properties of the rock- bolt material using the shear-lag method. Then, Bobet and Einstein (2011) discussed the importance of few parameters on the performance of grouted rockbolts, and introduced a formulation for mechanical contribution of the rockbolts based on shear interaction stress on the bolt surface. Carranza-Torres (2009) introduced a dimensionless coefficient named as "ground reinforcement- stiffness" (the contrast of stiffnesses of ground and rockbolt) which was a function of another coefficient named as reinforcement- density (the ratio of cross sectional area of rockbolt to the tributary area of rockbolt). These coefficients were used as the multipliers to obtain the confinement stress of composite material. Grasso et al. (1989) and Bernaud et al. (2009) works are also the other attempts to model the composite material properties.

All above mentioned researches have been performed for the passive grouted rockbolts except the works by Carranza-Torres (2009) and Bobet and Einstein (2011) in which pre-tensioned grouted rockbolts have been also considered. In the other attempt, Fahimifar and Ranjbarnia (2009) presented an analytical approach for these types of rockbolts based on the extension of the

works by Stille et al. (1989) and Fahimifar and Soroush (2005) having originally been carried out for the passive types. In that study, it was assumed; due to applying compression pressure by the bolt around tunnel, the rock mass become stronger than the broken rock mass. Accordingly, the presence of pre-tensioned force leads to development of greater confinement stress, and hence; the associated material would be much stronger.

In the second group, which the reinforcement contribution is in the form of a radial load spread uniformly within the zone of influence of the rockbolt, a comprehensive series of studies have been also conducted (Aydan, 1989; Peila & Oreste, 1995, 1996; Li & Stillborg, 1999; Oreste, 2003, 2004, 2008, 2009; Cai et al., 2004a, b; Guan et al., 2007; Bobet & Einstein, 2011). However, like the first group methods, a few of them have been devoted to the pre-tensioned grouted rockbolts such as the work by Bobet and Einstein (2011), Ranjbarnia, Oreste and Fahimifar (2016) with great limitations which will be discussed in the following.

In order to model the pre-tensioned grouted rockbolts as a systematic support of tunnels (at least in short-time), the relation between the value of pre-tensioned pressure on the tunnel surface (produced by the pre-tensioned force) and that of the fictitious constrained radial pressure by proximity of the face should be specially taken into consideration (Ranjbarnia et al., 2015). The advancement of tunnel face in front of bolted section leads to diminish the constrained radial pressure to zero and ultimately, the pre-tensioned pressure will only remain in that section. Providing the value of pre-tensioned pressure on the tunnel surface is greater than that of the constrained radial pressure, advancement of the tunnel face will not change the stresses within the rock mass around tunnel, and the ultimate load will not be greater than the initial tensioning. Conversely, providing the value of pre-tensioned pressure is less than that of constrained radial pressure, the stresses around tunnel will redistribute, and tunnel convergence will occur immediately after the radial pressure becomes less than the initial value prior to bolt installation, and hence; the bolt force will increase.

The above-mentioned analytical approaches for the pre-tensioned grouted rockbolts are not comprehensive solution. Because, the relation between the pre-tensioned and the constrained pressures is neglected (Carranza-Torres, 2009; Fahimifar & Ranjbarnia, 2009; Bobet & Einstein, 2011). Furthermore, it would be almost impossible to extend and modify the approaches to use for pre-tensioned types, and to realistically model the influence of pre-tensioned load. On the other hand, the widely available commercial finite-element and finite-difference computer codes, while in principle are capable of modeling the pre-tensioning, are not yet treating a solution to include the above discussion (about the relation of the pre-tensioned and the constrained pressures).

For this reason, this paper develops analytical approaches that have the following attributes

- It quantitatively models the efficiency of the pre-tensioning of grouted rockbolts in terms of reduction in both the tunnel convergence and failure zone around tunnel in comparison with the passive systems. In other words, it provides a solution for obtaining the optimum efficiency of the reinforced system in terms of the advancement of tunnel face (delay in installation), rockbolt arrangement, and the magnitude of pre-tensioning load e.g. the optimum pre-tensioning force for a given delay installation time and the rockbolt arrangement.
- It provides total length of the bolt in terms of the rockbolt arrangement and the magnitude of pre-tensioned load.

The present paper develops two analytical approaches on the basis of two described groups of methods by the assumption of rigid connection between the bolt and the rock mass. The formula-

tions of both methods are derived on the basis of convergence- confinement method representing the response of a reinforced circular tunnel under uniform in-situ stresses by a systematically installed pre-tensioned grouted rockbolts.

2. Problem definition

A circular tunnel of radius r_i is driven in a homogeneous, isotropic, initially elastic rock mass subjected to a hydrostatic stress field, p_0. When the rockbolts are installed, it is assumed, a certain convergence of tunnel has already been occurred and an initial plastic zone of radius $\bar{r}_e$ will develop around the tunnel (Fig. 1) (Ranjbarnia et al., 2014a). In this condition, there is a radial pressure on tunnel periphery supplied by proximity of the face, and its value is a percentage of field stress p_0 ($p_i = \beta \cdot p_0$), $0 < \beta < 1$). The magnitude of β is mainly dependent upon the distance from the tunnel face within influence limit of tunnel face (which is about two tunnel diameters beyond working face).

The pre-tensioned grouted rockbolt installation consists of placing a grouted anchor, tensioning the rockbolt and tying end of the bolt by nut and plate to the tunnel surface, and then grouting the reminder of the bolt length as (Fig. 2a) (Ranjbarnia et al., 2014a, 2015). The pre-tensioned force applied by the bolt plate to tunnel surface develops the radial pressure extending within

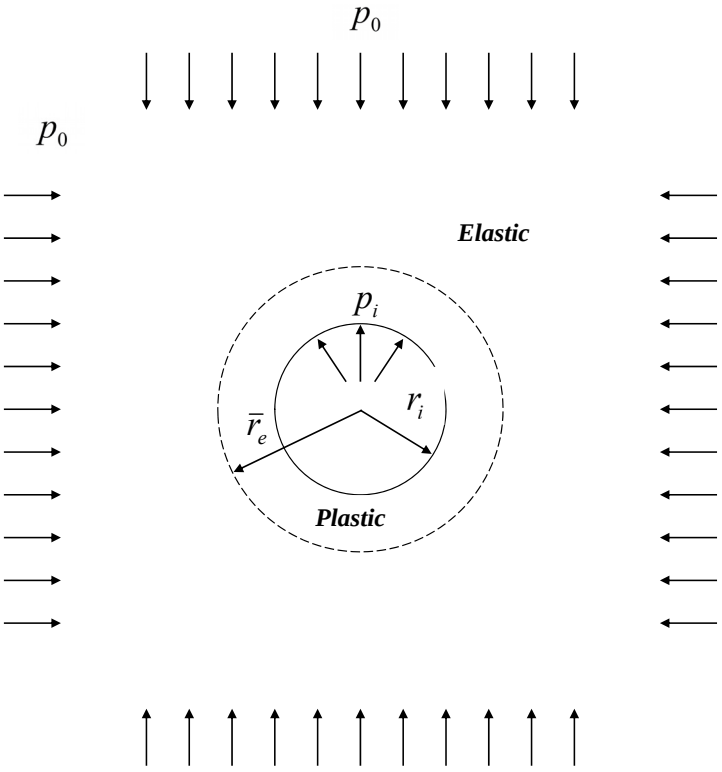

Fig. 1. The axisymmetric tunnel problem

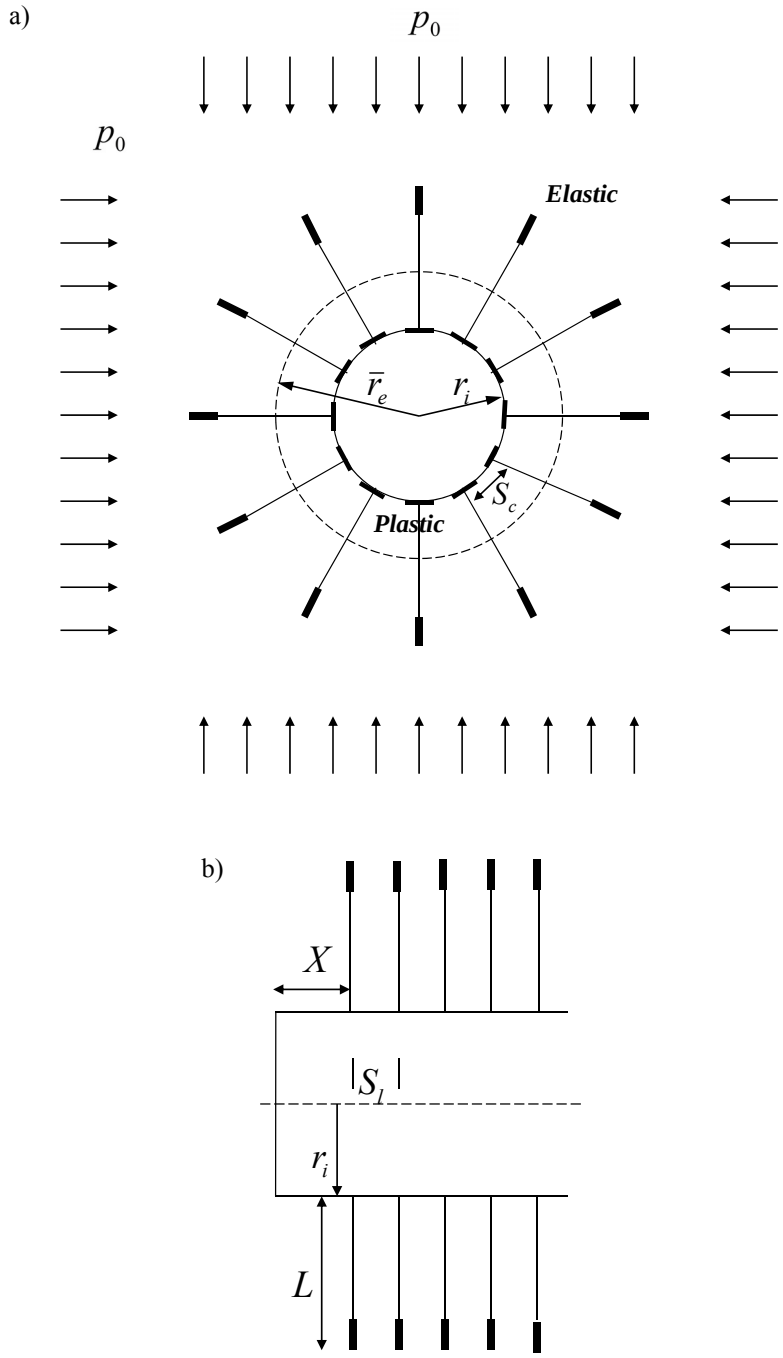

Fig. 2. Rockbolts arrangement (a) circular tunnel reinforced by systematic pre-tensioned grouted bolts; circumferential space between bolts (redrawn by Ranjbarnia et al. (2015))
(b) longitudinal spacing between bolts

the rock mass in the radial direction. As the bolts are installed systematically (Figs 2a and 2b), it is assumed, each bolt increases radial pressure within the influence domain of itself. Therefore (Ranjbarnia et al., 2014a, 2015)

$$p_{pre-ten} = \frac{T_{pre-ten}}{S_l \cdot S_{c_0}} \tag{1}$$

where $T_{pre-ten}$ and $p_{pre-ten}$ are the pre-tensioned force and its associated radial pressure at tunnel surface, respectively. S_l and S_{c_0} are longitudinal and circumferential bolts' spacing at tunnel surface, respectively.

It is assumed that the pre-tensioned force provides equivalent radial stress in domain zone of each bolt (Fig. 3) (Ranjbarnia et al., 2014a, 2015).

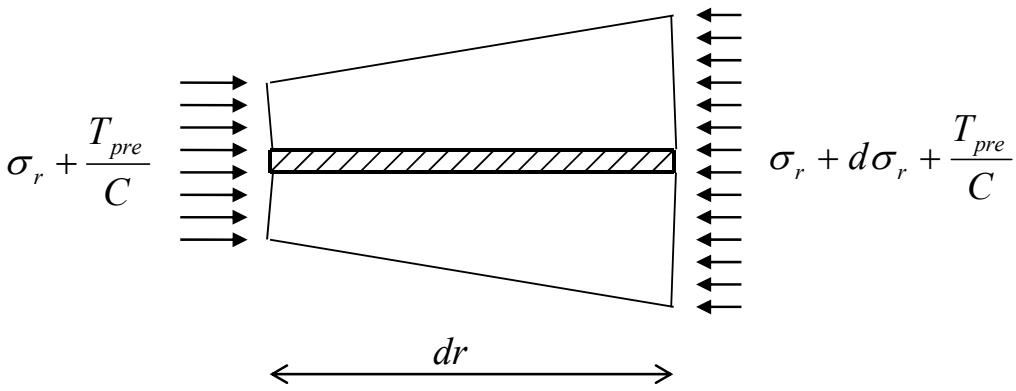

Fig. 3. Equivalent radial stress due to pre-tensioned load

After installing the bolts, as tunnel face is again advancing within the influence limit of the working face, the fictitious constrained radial stress will be further reduced and will be ultimately diminished. If the magnitude of constrained radial stress is less than that of the pre-tensioned pressure (*Case I*), progressive advancement of tunnel face and then full diminishing of the constrained radial stress will not lead to further radial displacement. This is because; by applying the pre-tensioned pressure, the overall radial stress on tunnel surface after full diminishing of the constrained stress is greater than that of its initial value prior to the bolt installation moment. Hence, the final bolt force is not greater than the initial applied tension i.e. the bolt force will remain constant and will be equal to pre-tensioned force, and grouting the reminder of bolt length has no influence on its behavior mechanism, but will only protect the bolt from corrosion. In this case, the bolt behavior is similar to support systems e.g. un-grouted tensioned bolts in which the bolt and the rock mass act independently.

However, if the magnitude of constrained radial stress is greater than that of pre-tensioned pressure (*Case II*), after somewhat diminishing of the constrained radial stress, the overall radial stress on tunnel surface will start to become less than that of its initial value prior to bolt installation. Thus, continuing excavation process will lead to further radial displacement of the surrounding rock mass and increase in the shear stresses between the bolt and the rock mass.

That is, the bolt force will increase till to full diminishing of the constrained radial stress, and the plastic radius becomes greater (Fig. 4). In this case, the bolt interacts by its surrounding medium i.e. the bolt does not act independently of the rock mass, and hence; their deformations cannot be separated.

For simplicity, further assumptions are made as follows:

- The problem is studied under plane-strain conditions; thus the three-dimensional effect even near the tunnel face is disregarded. That is, the analysis considers a 'slice' of tunnel of unit length i.e. 1 m along the axis of the tunnel or else the bolt properties should be adapted for a unit length.
- Rigid connection is assumed between the bolt and the rock. Therefore, the bolt force (both of pre-tensioned and probable ultimate force) provides a uniform radial support pressure in tunnel boundary and within the rock mass.
- The bolt has a length that it is anchored beyond the boundary of the broken zone in the original rock mass for both *Cases* of *I* and *II* (Figs 2a and 4).
- The pre-tensioned force applied to a rockbolt is typically a significant fraction of the bolt's yielding capacity. However, its magnitude is not a value leading the bolt to yield.

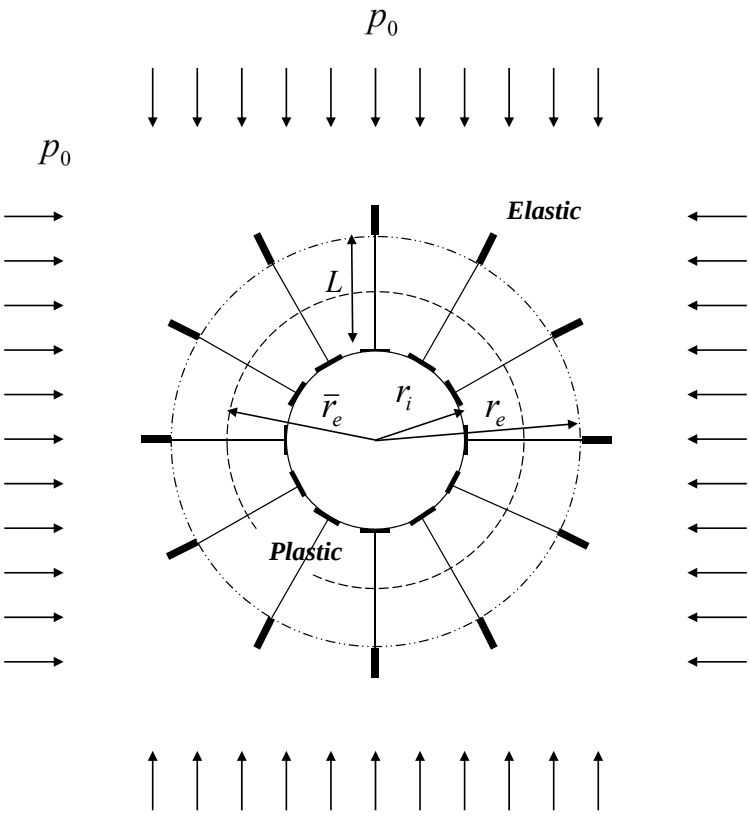

Fig. 4. Increasing tunnel plastic radius (redrawn by Ranjbarnia et al. (2015))

Also reminding again that

- Tunnel closure is only assumed due to advancement of the working face. In other words, short-term movements of rock mass are taken into account, and time-dependent properties of the rock mass are neglected.
- The influence of the weight of the rock in the plastic zone on tunnel displacements is disregarded.

3. The reinforcement mechanics of systematic pre-tensioned bolts

The analytical solutions are proposed to model the pre-tensioned grouted rockbolts behavior in circular tunnels on the basis of both described methods.

3.1. The first method

As mentioned in *Introduction*, in this method, the properties of the medium surrounding the tunnel is considered as an improved stronger material than the broken rock mass. To model the composite material properties, it will be worth figuring out the functional behavior of grouted rockbolt and its surrounding rock mass.

In general, the grouted rockbolts assist the rock mass to form a self supporting rock structure. They reinforce and mobilize the inherent strength of the rock mass by offering internal and confining pressure (Huang, 2002). Therefore, it is assumed in this paper, the grouted rockbolts reduce and control tunnel convergence through increasing the radial stress within the plastic rock mass. In other words, as the rockbolt restrains the deformation of rock mass, a tensioned force in the rockbolt results in, and at the same time, it applies pressure to the rock mass. Therefore, the adjusted radial stress of the composite material is written by

$$\sigma_r' = \sigma_r - \frac{T}{C} \tag{2}$$

where σ_r' is the adjusted radial stress for composite material, T is the overall rockbolt tension force, and C is the rockbolt effective area calculated by (Fig. 2)

$$C = S_l \cdot S_c \tag{3}$$

$$C = C_0 \cdot \frac{r}{r_i} \qquad r_i \le r \le r_i + L \tag{4}$$

where C_0 is the rockbolt effective area at tunnel surface, L is the bolt length located in the plastic zone, and r is a variable showing the radial distance from tunnel center. Substituting Equation (4) into Equation (2) gives

$$\sigma_r' = \sigma_r - \frac{T}{C_0}\frac{r_i}{r} \tag{5}$$

In this paper, the Hoek- Brown strength criterion (Hoek & Brown, 1980) is adopted for original rock mass

$$\sigma_\theta = \sigma_r + \left(m \cdot \sigma_c \cdot \sigma_r + s \cdot \sigma_c^2 \right)^{\frac{1}{2}} \tag{6}$$

where σ_θ and σ_r are the circumferential and radial stresses, respectively. σ_c is uniaxial compressive strength of the intact rock material, and parameters m and s are rock mass constants depending on the nature of the rock mass and its geotechnical conditions. Equation (6) can be used for the rock mass strength before and after failure by using appropriate m and s.

Substituting the adjusted radial stress of composite material into Equation (6) gives the strength criterion of composite material i.e.

$$\sigma_\theta = \sigma'_r + \left(m \cdot \sigma_c \cdot \sigma'_r + s \cdot \sigma_c^2 \right)^{\frac{1}{2}} \tag{7}$$

Note that due to plane strain and the axial symmetry assumptions, the tangential and radial stresses, σ_θ and σ_r, will be principal stresses, σ_1 and σ_3, respectively. As well, due to the rigid connection assumption between bolt and its surrounding rock, presence of the bolts does not change the principal stress directions.

Substituting Equation (2) into Equation (7) gives

$$\sigma_\theta = \sigma_r + \left(m \cdot \sigma_c \cdot \left(\sigma_r - \frac{T}{C} \right) + s \cdot \sigma_c^2 \right)^{\frac{1}{2}} - \frac{T}{C} \tag{8}$$

The axial bolt force can be obtained by

$$T = A_b \cdot E_s \cdot \varepsilon_b \tag{9}$$

where A_b and E_s are bolt cross section area and the modulus of elasticity of bolt, respectively, and ε_b is axial bolt strain.

As explained in section 2, for *Case I*, continuing excavation process will not impose further radial tunnel convergence and the bolt force will remain constant and will be equal to pre-tensioned load, i.e.

$$\varepsilon_b = \varepsilon_{pre-ten} \tag{10}$$

and so forth

$$T = T_{pre-ten} \tag{11}$$

In this condition, tunnel convergence will be equal to its value prior to the bolt installation.

It should be noted that, according to the static equilibrium, the pre-tensioned load is constant along the bolt, and hence; its corresponding pressure applied along the bolt to its surrounding rock mass is uniform. However, this pressure within the rock mass is linearly decreased from the tunnel surface to the depth of rock mass due to the increasing the rockbolt effective area (Fig. 3).

$$p_{pre-ten} = \frac{T_{pre-ten}}{C_0} \frac{r_i}{r} \qquad r_i \le r \le r_i + L \tag{12}$$

where $p_{pre-ten}$ is the pre-tensioned pressure.

For *Case II*, further radial displacements of the rock mass after full diminishing of the constrained stress become less than that of the pre-tensioned pressure leading a further tension to be imposed to the rockbolt. The additional bolt strain will be the same as radial rock mass strain due to the rigid connection assumption between them. Therefore

$$\varepsilon_b = \varepsilon_{pre\text{–}ten} + \varepsilon'_r \tag{13}$$

where ε'_r is the radial strain within rock mass that takes place after installing the bolts.

Prior to installing the bolts, on the other hand, a certain radial displacement of rock mass has occurred i.e. the plastic displacement in the initial plastic zone, $\overline{r}_e$, and the elastic deformations in the greater plastic zone, r_e, have been already developed (Figure 4). Hence, Equation (13) can be rewritten as

$$\varepsilon_b = \begin{cases} \varepsilon_r - \overline{\varepsilon}_r + \varepsilon_{pre\text{–}ten} & r_i < r \le \overline{r}_e \\ \varepsilon_r - \varepsilon_r^e + \varepsilon_{pre\text{–}ten} & \overline{r}_e < r \le r_e \end{cases} \tag{14}$$

(Note: $r_e - r_i = L$)

where ε_r is total radial strain within plastic rock mass, $\overline{\varepsilon}_r$ and ε_r^e are the radial strain within the rock mass before installing the bolts in the initial and developed plastic zone, respectively. To obtain each of these radial strains, the rock mass stress-strain behavior is assumed elastic strain-softening which is more appropriate behavior of most rock masses in tunnelling design (Hoek & Brown, 1997). Different approaches and formula have been presented to distribute stress and strain around tunnel for this behaviour (Brown et al., 1983; Alonso et al., 2003; Park et al., 2008; Lee & Pietruszczak, 2008; Wang et al., 2010; Ranjbarnia et al., 2014b)

However, as the aim of this paper is only to assess the critical and the effective parameters of the pre-tensioned grouted rockbolts, Brown et al. (1983) work (one of the simplest models) is used although it does not have very exact predictions (Alonso et al., 2003). The rockbolts parameters implemented into this approach is presented in Appendix 1 in the form of calculation sequence to obtain Ground Response Curve of reinforced tunnel.

Differential equation of equilibrium of original rock mass around tunnel at radius r from the tunnel centre in polar coordinates is given by

$$\frac{d\sigma_r}{dr} = \frac{\sigma_\theta - \sigma_r}{r} \tag{15}$$

Substituting the composite material criterion into Equation (15) results in the differential equation of equilibrium for the stronger rock mass

$$\frac{d\sigma_r}{dr} = \frac{\left(m \cdot \sigma_c \cdot \left(\sigma_r - \frac{T}{C} \right) + s \cdot \sigma_c^2 \right)^{\frac{1}{2}} - \frac{T}{C}}{r} \tag{16}$$

or

$$\frac{d\sigma_r}{dr} = \frac{\left(m \cdot \sigma_c \cdot \left(\sigma_r - \frac{T}{C_0}\chi \right) + s \cdot \sigma_c^2 \right)^{\frac{1}{2}} - \frac{T}{C_0}\chi}{r} \tag{17}$$

in which

$$\chi = \frac{r_i}{r} \tag{18}$$

For *Case I*, the ultimate tunnel convergence will be identical to that of the installing time. However, Equation (17) can be extended to this condition as follows

$$\frac{d\sigma_r}{dr} = \frac{\left(m \cdot \sigma_c \cdot \left(\sigma_r - \frac{A_b \cdot E_s \cdot \varepsilon_{pre-ten}}{C_0}\chi\right) + s \cdot \sigma_c^2\right)^{\frac{1}{2}} - \frac{A_b \cdot E_s \cdot \varepsilon_{pre-ten}}{C_0}\chi}{r} \tag{19}$$

And for *Case II*

$$\frac{d\sigma_r}{dr} = \frac{\left(m \cdot \sigma_c \cdot \left(\sigma_r - \frac{A_b \cdot E_s \cdot \left(\varepsilon_r - \bar{\varepsilon}_r + \varepsilon_{pre-ten}\right)}{C_0}\chi\right) + s \cdot \sigma_c^2\right)^{\frac{1}{2}} + \frac{A_b \cdot E_s \cdot \left(\varepsilon_r - \bar{\varepsilon}_r + \varepsilon_{pre-ten}\right)}{C_0}\chi}{r} \qquad r_i \le r \le \bar{r}_e \tag{20}$$

and

$$\frac{d\sigma_r}{dr} = \frac{\left(m \cdot \sigma_c \cdot \left(\sigma_r - \frac{A_b \cdot E_s \cdot \left(\varepsilon_r - \varepsilon_r^e + \varepsilon_{pre-ten}\right)}{C_0}\chi\right) + s \cdot \sigma_c^2\right)^{\frac{1}{2}} + \frac{A_b \cdot E_s \cdot \left(\varepsilon_r - \varepsilon_r^e + \varepsilon_{pre-ten}\right)}{C_0}\chi}{r} \qquad \bar{r}_e < r \le r_e \tag{21}$$

The differential Equation (19) has both boundary conditions of (1) and (2), while Equations (20) and (21) have boundary condition (1) and (2), respectively:

(1) At $r = r_i$, $\sigma_r = p_i$ in which r_i is the tunnel radius and p_i is the magnitude of radial pressure in the tunnel surface.

(2) At $r = r_e$, $\sigma_r = \sigma_{re}$, in which σ_{re} is the radial stress at the outer boundary of plastic zone and is obtained as follows (Brown et al., 1983)

$$\sigma_{re} = p_0 - M \cdot \sigma_c \tag{22}$$

in which

$$M = \frac{1}{2}\left[\left(\frac{m}{4}\right)^2 + m\frac{p_0}{\sigma_c} + s\right]^{1/2} - \frac{m}{8} \tag{23}$$

To plot Ground Response Curve or to calculate the ultimate radial convergence, the radial stress should be reduced to zero. This is because, in the first method, the material surrounding the tunnel is only considered as a stronger material and GRC of a stronger material is to be calculated.

These differential equations can be solved by numerical method due to their algebraic complexity. An iterative finite difference solution on the basis of Brown et al. (1983) work is used. That is, the plastic zone is split into annular rings and calculations are starting from the unknown elastic-plastic interface towards the tunnel by incrementing the tangential strain value for each calculation step and then calculating the corresponding radial strain (Brown et al., 1983)

If equation (19) is rewritten for a ring $r_{(j)}$, it can be

$$\frac{\sigma_{r(j-1)}-\sigma_{r(j)}}{r_{(j-1)}-r_{(j)}}=\frac{\left[\frac{m_a\sigma_c}{2}\left[\begin{array}{l}\left(\sigma_{r(j-1)}+\sigma_{r(j)}\right)+\\ -\frac{A_bE_s}{C_0}\left(\varepsilon_{pre-ten(j-1)}+\varepsilon_{pre-ten(j)}\right)\chi_a\end{array}\right]+s_a\sigma_c^2\right]^{1/2}}{\frac{r_{(j-1)}+r_{(j)}}{2}}+$$
$$-\frac{A_bE_s}{C_0}\frac{\left(\varepsilon_{pre-ten(j-1)}+\varepsilon_{pre-ten(j)}\right)}{r_{(j-1)}+r_{(j)}}\chi_a \tag{24}$$

in which

$$\chi_a=\frac{r_i}{\frac{r_{(j)}+r_{(j-1)}}{2}}$$
$$m_a=\frac{m_{(j-1)}+m_{(j)}}{2}$$
$$s_a=\frac{s_{(j-1)}+s_{(j)}}{2} \tag{25}$$

Note that the average value of parameters in the right hand side of Equation (19) (i.e. m, s, r, σ_r) were written in Equation (24) e.g. m_a is the average value of m at two rings $r_{(j-1)}$ and $r_{(j)}$.

where different parameters are in $r_{(j-1)}$ and $r_{(j)}$ radii.

Defining some parameters and making simplifications results in the second order equation giving $\sigma_{r(j)}$

$$a\cdot\sigma_{r(j)}^2+b\cdot\sigma_{r(j)}+c=0 \tag{26}$$

and solution is

$$\sigma_{r(j)}=\frac{-b-\sqrt{b^2-4ac}}{2a} \tag{27}$$

in which

$$a^*=\frac{1}{4K^2}\qquad b^*=\frac{-K_{pre-ten}}{K}-\frac{\sigma_{r(j-1)}}{2K^2}-2K_2$$
$$c^*=\sigma_{r(j-1)}\left[\frac{\sigma_{r(j-1)}}{4K^2}+\frac{K_{pre-ten}}{K_2}-2K_2\right]+\left(K_{pre-ten}\right)^2+4\left(K_2K_{pre-ten}\right)-s_a\sigma_c^2 \tag{28}$$

where

$$\lambda_{(j)} = \frac{r_{(j)}}{r_e} \tag{29}$$

$$K = \frac{\lambda_{(j-1)} - \lambda_{(j)}}{\lambda_{(j)} + \lambda_{(j-1)}} \tag{30}$$

$$K_2 = \frac{m_a \sigma_c}{4} \tag{31}$$

$$\gamma_{pre-ten} = \varepsilon_{pre-ten(j-1)} + \varepsilon_{pre-ten(j)} = 2\varepsilon_{pre-ten(j)} = 2\varepsilon_{pre-ten} \tag{32}$$

$$K_{pre-ten} = \frac{A_b E_s}{2C_0} \gamma_{pre-ten} \cdot \chi_a \tag{33}$$

Performing the same process for both Equations (20) and (21) changes the multiplier of second order as follows
for $r_i \le r \le \bar{r}_e$ zone

$$a^* = \frac{1}{4K^2}, \qquad b^* = \frac{\bar{K}_1^* - K_1^* - K_{pre-ten}}{K} - \frac{\sigma_{r(j-1)}}{2K^2} - 2K_2$$

$$c^* = \sigma_{r(j-1)} \left[\frac{\sigma_{r(j-1)}}{4K^2} + \frac{K_1^* - \bar{K}_1^* + K_{pre-ten}}{K_2} - 2K_2 \right] +$$
$$+ \left(K_1^* - \bar{K}_1^* + K_{pre-ten} \right)^2 + 4\left(K_1^* K_2 - \bar{K}_1^* K_2 + K_2 K_{pre-ten} \right) - s_a \sigma_c^2 \tag{34}$$

where

$$\gamma^* = \varepsilon_{r(j-1)} + \varepsilon_{r(j)} \tag{35}$$

$$K_1^* = \frac{A_b E_s}{2C_0} \gamma^* \chi_a \tag{36}$$

$$\bar{\gamma}^* = \bar{\varepsilon}_{r(j-1)} + \bar{\varepsilon}_{r(j)} \tag{37}$$

$$\bar{K}_1^* = \frac{A_b E_s}{2C_0} \bar{\gamma}^* \chi_a \tag{38}$$

and for $\bar{r}_e < r \le r_e$ zone

$$a^* = \frac{1}{4K^2}, \qquad b^* = \frac{K^{e(*)} - K_1^* + K_{pre-ten}}{K} - \frac{\sigma_{r(j-1)}}{2K^2} - 2K_2$$

$$c^* = \sigma_{r(j-1)}\left[\frac{\sigma_{r(j-1)}}{4K^2} + \frac{K_1^* - K^{e(*)}}{K_2} - 2K_2\right] + \left(K_1^* - K^{e(*)} + K_{pre-ten}\right)^2 +$$
$$+4\left(K_1^* K_2 - K^{e(*)} K_2 + K_2 K_{pre-ten}\right) - s_a \sigma_c^2 \tag{39}$$

where

$$K_e = \frac{A_b E_s}{2C_0}\gamma_e \chi_a \tag{40}$$

$$\gamma_e = \varepsilon_{r(j-1)}^e + \varepsilon_{r(j)}^e = \alpha\left(\varepsilon_{re} + \varepsilon_{re}\right) = \zeta\frac{M\sigma_C}{G} \qquad 0 < \zeta < 1 \tag{41}$$

Note: superscript * refers to the first method.

3.2. The second method

As mentioned in *Introduction*, this method is on the basis of functional mechanism of grouted rockbolt in which reinforcement contribution is in the form of a radial load spread within its influencing zone. For tunnel with circular cross section, uniform in-situ stresses, and close spacing of the rockbolts, the differential equation of equilibrium is given as (Oreste, 2008)

$$\frac{d\sigma_r}{dr} = \frac{\sigma_\theta - \sigma_r}{r} + \frac{dT}{dr}\frac{1}{C} \tag{42a}$$

or

$$\frac{d\sigma_r}{dr} = \frac{\sigma_\theta - \sigma_r}{r} + \frac{dT}{dr}\frac{r_i}{C_0}\frac{1}{r} \tag{42b}$$

Substituting failure criterion of original rack mass i.e. Equation (6) into Equation (42b) gives

$$\frac{d\sigma_r}{dr} = \frac{\left[m\sigma_c\sigma_r + s\sigma_c^2\right]^{1/2}}{r} + \frac{dT}{dr}\frac{r_i}{r}\frac{1}{C_0} \tag{43}$$

The above differential equations have the same boundary conditions as Equations (19)-(21).

To solve differential equation for *Case I*, it is assumed that the radial pressure must be reduced from p_0 to $p_{pre-ten}$ in which $p_{pre-ten}$ is greater than $\beta \cdot p_0$ (the constrained stress at bolt installation time). That is, as the pre-tensioned pressure on tunnel surface $p_{pre-ten}$ is applied, it is added to $\beta \cdot p_0$ and then an outward radial elastic deformation occurs, and unloading takes place. Full diminishing of $\beta \cdot p_0$ associated with progressive advancement of tunnel face leads again to loading of the rock mass around tunnel and therefore, according to solid mechanics concepts, some inward radial elastic deformation occurs which its magnitude is dependent upon $p_{pre-ten}$ value. However, in this paper, small elastic deformations and variations of total deformations are disregarded in the formula, and hence; the ultimate radial convergence will almost be the same as that of the bolt installation time. The differential equation for this condition will be

$$\frac{d\sigma_r}{dr} = \frac{\sigma_\theta - \sigma_r}{r} \tag{44}$$

with the following boundary condition (Ranjbarnia et al., 2014a, 2015)

(1) At $r = r_i$, $\sigma_r = p_i$ in which $\beta \cdot p_0 \le p_i \le p_0$.

(2) At $r = r_e$, $\sigma_r = \sigma_{re}$.

From the mathematical point of view, on the other hand, as the load is constant along the bolt for *Case I*, dT/dr will be zero and Equation (44) will be obtained from Equation (43).

For *Case II*, after dwindling of the radial pressure on tunnel surface from the remained in-situ radial pressure i.e. $\beta \cdot p_0$ to pre-tensioned pressure i.e. $p_{pre-ten}$, the radial deformations of rock mass will increase, and further tensioned is imposed to the bolt. This process is continued till to full diminishing of the constrained stress $\beta \cdot p_0$, and till to decreasing the radial pressure on tunnel surface to $p_{pre-ten}$. Thus, the differential equation for this condition will be

$$\frac{d\sigma_r}{dr} = \frac{\sigma_\theta - \sigma_r}{r} + \frac{dT}{dr}\frac{r_i}{C_0}\frac{1}{r} \tag{45}$$

with the following boundary conditions

(1) At $r = r_i$, $\sigma_r = p_i$ in which $p_{pre-ten} \le p_i \le p_0$ (this is just for $r_i < r \le \bar{r}_e$ zone).

(2) At $r = r_e$, $\sigma_r = \sigma_{re}$ (this is just for $\bar{r}_e < r \le r_e$ zone).

Equation (45) can be rewritten as (Ranjbarnia et al., 2015)

$$\frac{\sigma_{r(j-1)} - \sigma_{r(j)}}{r_{(j-1)} - r_{(j)}} = \frac{\left[\frac{m_a\sigma_c}{2}\left(\sigma_{r(j)} + \sigma_{r(j-1)}\right) + s_a\sigma_c^2\right]^{1/2}}{\frac{r_{(j)} + r_{(j-1)}}{2}} + \\ + \frac{T_{(j-1)} - T_{(j)}}{r_{(j-1)} - r_{(j)}} \cdot \frac{r_i}{C_0} \cdot \frac{2}{r_{(j)} + r_{(j-1)}} \tag{46}$$

or

$$\frac{\sigma_{r(j-1)} - \sigma_{r(j)}}{r_{(j-1)} - r_{(j)}} = \frac{\left[\frac{m_a\sigma_c}{2}\left(\sigma_{r(j)} + \sigma_{r(j-1)}\right) + s_a\sigma_c^2\right]^{1/2}}{\frac{r_{(j)} + r_{(j-1)}}{2}} + \\ + \frac{A_b E_s \begin{pmatrix} \varepsilon_{r(j-1)} - \bar{\varepsilon}_{r(j-1)} + \varepsilon_{pre-ten(j-1)} + \\ -\varepsilon_{r(j)} + \bar{\varepsilon}_{r(j)} + \varepsilon_{pre-ten(j)} \end{pmatrix}}{r_{(j-1)} - r_{(j)}} \cdot \frac{r_i}{C_0} \cdot \frac{2}{r_{(j)} + r_{(j-1)}} \tag{47}$$

Processing Equation (47) in the similar way performed for Equations (19)-(21) gives the multiplier of second order, respectively as follows (Ranjbarnia et al., 2015)
for $r_i < r \le \bar{r}_e$ zone

$$a^{**} = \frac{1}{4K^2}, \qquad b^{**} = -\frac{K_1^{**} - \bar{K}_1^{**}}{K} - \frac{\sigma_{r(j-1)}}{2K^2} - 2K_2$$

$$c^{**} = \sigma_{r(j-1)}\left[\frac{\sigma_{r(j-1)}}{4K^2} + \frac{K_1^{**} - \bar{K}_1^{**}}{K} - 2K_2\right] + \left(K_1^{**} - \bar{K}_1^{**}\right)^2 - s_a\sigma_c^2 \tag{48}$$

where

$$\gamma^{**} = d\varepsilon_{r(j)} = \varepsilon_{r(j)} - \varepsilon_{r(j-1)} \tag{49}$$

$$K_1^{**} = \frac{A_b E_s r_i}{C_0\left(r_{(j-1)} - r_{(j)}\right)}\gamma^{**} \tag{50}$$

$$\bar{\gamma}^{**} = d\bar{\varepsilon}_{r(j)} = \bar{\varepsilon}_{r(j)} - \bar{\varepsilon}_{r(j-1)} \tag{51}$$

$$\bar{K}_1^{**} = \frac{A_b E_s r_i}{C_0\left(r_{(j-1)} - r_{(j)}\right)}\bar{\gamma}^{**} \tag{52}$$

and for $\bar{r}_e < r \le r_e$ zone

$$a^{**} = \frac{1}{4K^2}, \qquad b^{**} = -\frac{K_1^{**} - K_1^{e(**)}}{K} - \frac{\sigma_{r(j-1)}}{2K^2} - 2K_2$$

$$c^{**} = \sigma_{r(j-1)}\left[\frac{\sigma_{r(j-1)}}{4K^2} + \frac{K_1^{**} - K_1^{e(**)}}{K} - 2K_2\right] + \left(K_1^{**} - K_1^{e(**)}\right)^2 - s_a\sigma_c^2 \tag{53}$$

where

$$\gamma^{e(**)} = d\varepsilon_{r(j)}^{e} = \varepsilon_{r(j)}^{e} - \varepsilon_{r(j-1)}^{e} \tag{54}$$

$$K_1^{e(**)} = \frac{A_b E_s r_i}{C_0\left(r_{(j-1)} - r_{(j)}\right)}\gamma^{e(**)} \tag{55}$$

Note: superscript ** refers to the second method

4. Examples

Ground Response Curve calculations, for a rock mass being reinforced by the pre-tensioned grouted rockbolts, are performed by the proposed methods. To quantify the effect of pre-tensioning, GRC calculations are also performed for the passive grouted rockbolts. Other parameters such as

- the magnitude of pre-tensioned load and
- bolt's spacing

are investigated to identify the weight of each in tunnel stability. The examples were selected from (Ward et al., 1976; Brown et al., 1983)

Example 1. Verification of the proposed models results with that of to the Kielder experimental tunnel

According to Ward et al. (1976), total short-term movement of tunnel surface in the unsupported section of mudstone with weak engineering properties (Table 1) was about 8 mm in which less than 1 mm had occurred before the face reached, and about 6 mm when the face had advanced 2 m beyond this position. If the reinforcement system was installed just in front of the face, it can be expected that tunnel closure was about 1-2 mm prior to bolt installation (assumed value is 1.5 mm in this paper).

TABLE 1

Mechanical properties of mudstone in the Kielder experimental tunnel (Hoek & Brown, 1980)

Prarameter	Value
Axial compressive strength σ_c (MPa)	37
Radius of tunnel, r_i (m)	1.65
In-situ stress, p_0 (MPa)	2.56
Deformation modulus, E (MPa)	5000
Poisson's ratio of rock mass	0.25
Strength parameter, m peak	0.1
s peak	0.00008
m residual	0.05
S residual	0.00001
Dilation angle (degree)	10

Of the eight sections with different support systems in mudstone, one of them is only reinforced by passive grouted rockbolts (Table 2).

TABLE 2

Geometrical parameters of passive grouted rockbolts in the Kielder experimental tunnel (Hoek & Brown, 1980)

The parameter	The value
Fully grouted Rockbolt Length, L (m)	1.8
Young's modulus of rock bolt, E_s (GPa)	210
Bolt diameter, d_b (mm)	25
Distance between rockbolt, S_l * S_c (m2)	0.9 * 0.9

The corresponding ground response curves (Fig. 5) and output results (Table 3) show the calculated and measured deformations data at tunnel surface for supported and unsupported rock mass. As observed, the proposed methods can almost predict the identical results for the reinforced section, and agree, in a satisfactory way, with the in-situ measurements.

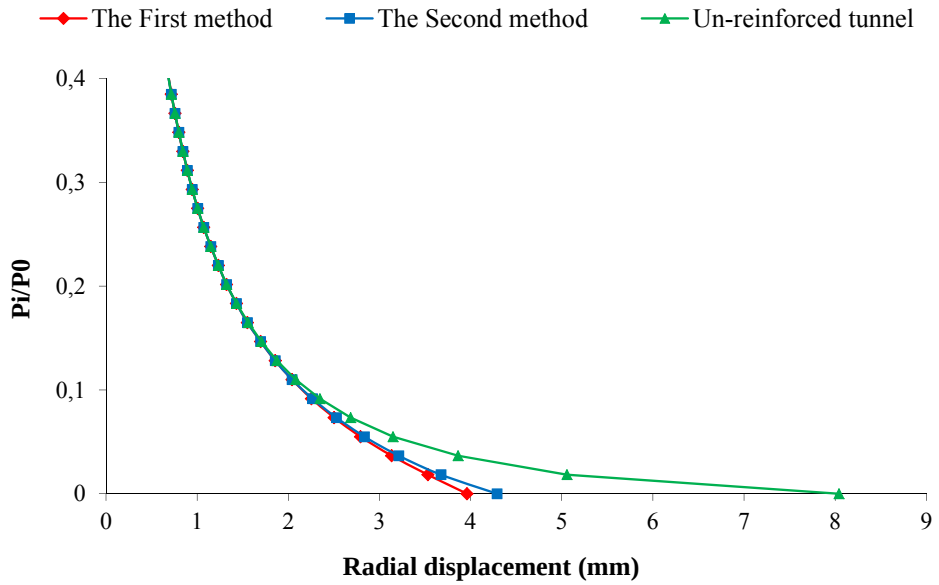

Fig. 5. Ground response curves for the rock mass around Kielder experimental tunnel

TABLE 3

The measured deformations by (Ward et al., 1976) and the calculated deformations by the proposed methods at the rock surface for supported and unsupported rock mass

Parameter	Measured	Calculated
Un-reinforced tunnel	8 mm	8.05 mm
Passive grouted bolt section	4-5 mm	4.27 mm (the first method)
		3.96 mm (the second method)

In continue; the parameters associated to pre-tensioned grouted rock bolts are investigated.

Note: the curves of GRC associated to the passive and the pre-tensioned reinforcements in Examples 2-5 are only calculated by the second method, meanwhile; the output results of both methods for these examples are available in Table 6.

Example 2. Evaluating the performance of grouted bolts for Case I circumstance

A highway tunnel with 10.7 m in diameter is driven in a fair to good quality limestone at a depth of 122 m below the surface (Brown et al., 1983) (Table 4).

TABLE 4

Mechanical properties of the rock mass (Brown et al., 1983) in Example 2-5

Prarameter	Value
Axial compressive strength σ_c (MPa)	27.6
Radius of tunnel, r_i (m)	5.35
In-situ stress, p_0 (MPa)	3.31
Deformation modulus, E (MPa)	1380
Poisson's ratio of rock mass	0.25
Strength parameter, m peak	0.5
s peak	0.001
m residual	0.1
S residual	0
Dilation coefficients, f	1.2
h	2
α	3.5

The pre-tensioned grouted rockbolts are installed for $T_{pre-ten}$ =17 ton. As can be calculated (Table 5), the pre-tensioned pressure is greater than the fictitious constrained pressure of tunnel face. Consequently, the circumstance of *Case I* will take place i.e. continuing excavation process will not induce any further tunnel convergence.

TABLE 5

Geometrical parameters of reinforcement systems in Examples 2-5

Example	**Rockbolt Density (m^2)**	**pre-tensioned force (ton)**	**constrained pressure due to working face**
2A*		17	16.5 ton/m^2 (0.165 MPa)
2P*	$C_0 = 1$	0	16.5 ton/m^2 (0.165 MPa)
3A	$C_0 = 1$	17	33.1 ton/m^2 (0.331 MPa)
3P	$C_0 = 0.5$	0	33.1 ton/m^2 (0.331 MPa)
4A	$C_0 = 0.5$	17	33.1 ton/m^2 (0.331 MPa)
4P	$C_0 = 0.5$	0	33.1 ton/m^2 (0.331 MPa)
5AI	$C_0 = 1$	21.25	33.1 ton/m^2 (0.331 MPa)
5AII	$C_0 = 0.75$	17	33.1 ton/m^2 (0.331 MPa)
5AIII	$C_0 = 1$	22.67	33.1 ton/m^2 (0.331 MPa)

* Letters A and P in the examples denote the employing of active (pre-tensioned) and passive grouted rockbolt, respectively.
Note: The diameter of bolts in all examples is 25 mm.

The output results (Fig. 6 and Table 6) show the efficiency of pre-tensioning. The convergence of tunnel by pre-tensioning of bolts is reduced considerably.

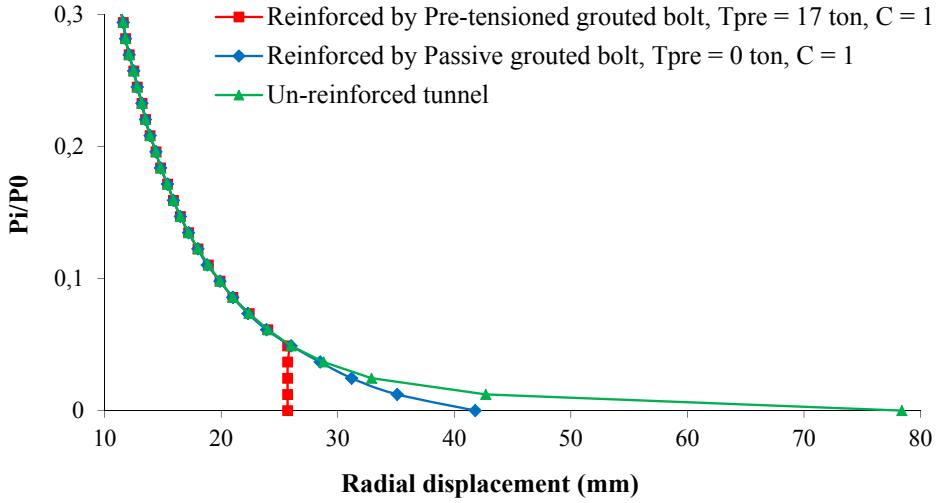

Fig. 6. Ground response curve for the rock mass around tunnel in Examples 2

TABLE 6

The output results of Example 2-4

Example	Approach	Ultimate convergence of tunnel reinforced by …. *		Plastic radius of tunnel reinforced by …. **	
		Pre-tensioned bolt	Passive bolt	Pre-tensioned	Passive
2	The first method	28.1	36.2	8.24	9.06
	The second method	25.7	41.8	7.96	9.56
3	The first method	25.5	31.2	7.94	8.57
	The second method	24.7	35	7.84	8.94
4	The first method	23.1	28.6	7.64	8.3
	The second method	19.5	29.5	7.15	8.39
Unreinforced tunnel		78.4		12.27	

* unit is millimetre
**unit is metre

Example 3. Evaluating the performance of grouted bolts for Case II circumstance

If the pre-tensioned grouted rockbolts in Example 2 are installed sooner i.e. at section where $p_i = 0.1\ p_0 = 33.1$ ton/m^2, the circumstance of *Case I* will take place.

Comparing the results of 3A and 3P (Table 6 and Fig. 7), the result shows that employing the pre-tensioned grouted rockbolts will not be as efficiency as the previous circumstances in Example 2A (*Case I*). Hence, the less delay to install the bolt, the less need to apply the pre-tensioned load.

On the other hand, if the bolts are installed with great delay i.e. the tunnel advancement is so long that insignificant and least constrained radial pressure of tunnel head is remained prior to bolt installation, the bolt may be much pre-tensioned to apply greater initial pressure to the

tunnel surface (trying to alter or close the condition from *Case II* to *Case I*). However, it may lead to bolts with a final load too close to yield.

Reducing spacing of bolts may be an appropriate alternative for pre-tensioning of bolts to confine tunnel convergence in case increasing pre-tensioned force is impossible and is insufficient or else the bolt will yield. Example 4 evaluates this issue.

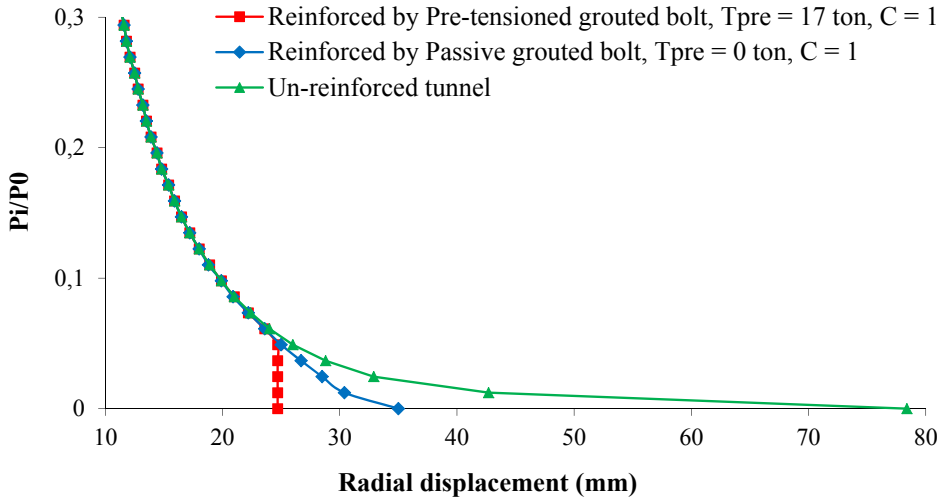

Fig. 7. Ground response curve for the rock mass around tunnel in Examples 3

Example 4. Evaluating the influence of bolts density in the performance of pre-tensioned grouted bolts in tunnel stabilization

In this example, the effect of rockbolt density is evaluated. Pre-tensioned grouted rockbolts in Example 3 are installed with $C_0 = 0.5$ m^2. In this case, the circumstance of *Case I* is produced, and the convergence will be significantly reduced in comparison to employing of passive grouted bolts (Table 6 and Fig. 8).

Example 5. Comparing the increase of bolt density parameter with the increase of pre-tensioned force in tunnel stabilization

The weighting of spacing of bolts and increasing the pre-tensioned force which both increase the radial pressure are quantified and compared. Both parameters variations have the identical influence on confining of the convergence and stability of tunnel provided they lead *Case I* to occur. However, if the pre-tension force is increased by α percent, the ratio of new corresponding pressure to the radial constrained pressure on tunnel surface will be

$$\frac{p_{i,new}}{p_i} = \frac{(1+\alpha)\cdot\dfrac{T_{pre-ten}}{C_0}}{\dfrac{T_{pre-ten}}{C_0}} = (1+\alpha) \tag{58a}$$

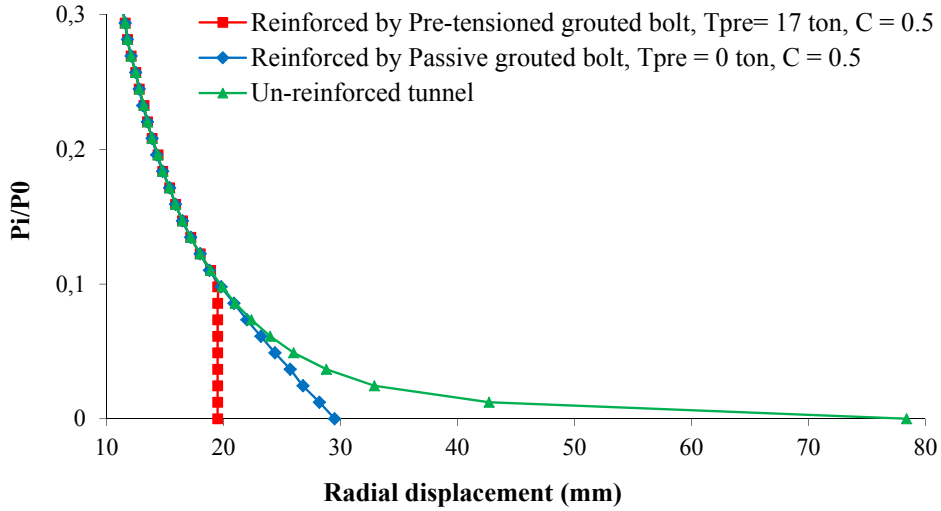

Fig. 8. Ground response curve for the rock mass around tunnel in Examples 4

or

$$p_{i,new} = (1+\alpha)p_i \tag{58b}$$

On the other hand, reducing bolts' spacing as α percent gives the following result for tunnel surface pressure

$$\frac{p'_{i,new}}{p_i} = \frac{\frac{T_{pre-ten}}{(1-\alpha)\cdot C_0}}{\frac{T_{pre-ten}}{C_0}} = \frac{1}{(1-\alpha)} \tag{59a}$$

or

$$p'_{i,new} = \frac{p_i}{(1-\alpha)} \tag{59b}$$

Comparing the Equations (58b) and (59b) gives

$$p'_{i,new} > p_{i,new} \tag{60}$$

Therefore, it can be concluded that reducing spacing of bolts is more effective than increasing of the pre-tensioned force. On the other hand, this parameter has great influence on confining convergence in the case of passive grouted rockbolts. This is because; it reflects the reinforcement density in the rock mass. In other words, reducing spacing of bolts not only efficiently increases tunnel surface pressure but also effectively improves broken rock mass strength.

In this Example, the pressure on tunnel surface is increased up to 25% either of the pre-tensioned force or the rockbolt density. As output results show (Table 7 and Fig. 9), the rockbolt density has more effect in tunnel stability than the pre-tensioned force. This is because; the radial

pressure will be greater while increasing rockbolt density. However, if the pressure on tunnel wall is improved by increasing the pre-tensioned force to the magnitude achieved by increasing rockbolt density i.e. $p_{pre-ten}$ = 22.67 ton/m^2, the supporting performance of bolts will not be as effective as the case of increase in the bolt density (Example 5AII and 5AIII).

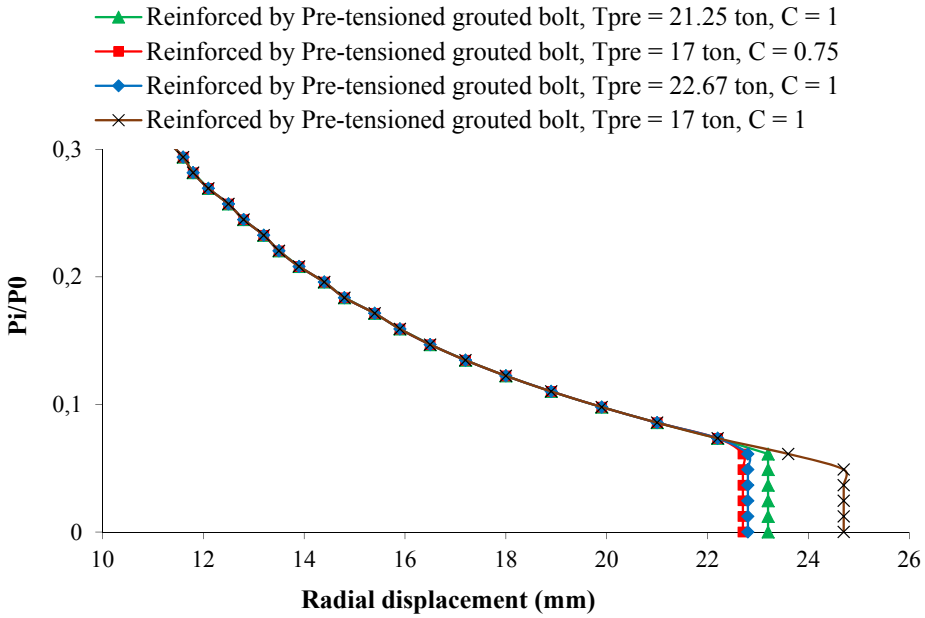

Fig. 9. Ground response curve for the rock mass around tunnel in Example 5

TABLE 7

The output results of Example 5

Example	Ultimate convergence (mm)	Plastic radius (m)
3	24.7	7.84
5AI	23.2	7.69
5AII	22.7	7.58
5AIII	22.8	7.6

5. Conclusions

Two new analytical approaches were proposed for the computation of the Ground Response Curve of a circular tunnel reinforced by the pre-tensioned grouted rockbolts, and also computation of ultimate plastic zone around tunnel. These models were developed on the basis of short-term convergence of tunnel i.e. tunnel convergence would only occur in term of reducing the constrained stress on surface due to tunnel face advancement. Consequently, the value of the constrained radial stress at bolt installation time and applied pre-tensioned pressure on tunnel were focused on in process of modeling.

Different examples were solved by these approaches. The results obtained through these two models were almost identical and comparable. The results showed pre-tensioning of grouted rockbolts will be very appropriate option when installation of rockbolts is carried out with delay.

References

Alonso E., Alejano L.R., Varas F., Fdez.-Manin G., Carranza-Torres C., 2003. *Ground reaction curves for rock masses exhibiting strain-softening behaviour*. International Journal for Numerical and Analytical Methods in Geomechanics, 27, 13, 1153-1185.

Aydan Ö., 1989. *The stabilisation of rock engineering structures by rockbolts*. Ph.D. Thesis, Nagoya University.

Bernaud D., Maghous S., Buhan P., Couto E., 2009. *A numerical approach for design of bolt-supported tunnels regarded as homogenized structures*. Tunnelling and Underground Space Technology, 24, 5, 533-546.

Bobet A., 2006. *A simple method for analysis of point anchored rockbolts in circular tunnels in elastic ground*. Rock Mechanics and Rock Engineering, 39, 4, 315- 338.

Bobet A., Einstein E., 2011. *Tunnel reinforcement with rockbolts*. Tunnelling and Underground Space Technology, 26, 1, 100-123.

Brown E.T., Bray J.W., Ladanyi B., Hoek E., 1983. *Ground response curves for rock tunnels.* Journal Geotechnical Engineering, 109, 1, 15-39.

Carranza-Torres C., 2009. *Analytical and numerical study of the mechanics of rockbolt reinforcement around tunnels in rock masses*. Rock Mechanics and Rock Engineering, 42, 2, 175-228.

Cai Y., Esaki T., Jiang Y., 2004a. *An analytical model to predict axial load in grouted rock bolt for soft rock tunnelling*. Tunnelling and Underground Space Technology, 19, 6, 607-618.

Cai Y., Jiang Y., Esaki T., 2004b. *A rock bolt and rock mass interaction model*. International Journal of Rock Mechanics and Mining Science, 41, 7, 1055-1067.

Fahimifar A., Soroush H., 2005. *A theoretical approach for analysis of the interaction between grouted rockbolts and rock masses*. Tunnelling and Underground Space Technology, 20, 4, 333-343.

Fahimifar A., Ranjbarnia M., 2009. *Analytical approach for the design of active grouted rockbolts in tunnel stability based on convergence-confinement method.* Tunnelling and Underground Space Technology, 24, 4, 363-375.

Grasso P.G., Mahtab A., Pelizza S., 1989. *Riqualificazione della massa roccoisa: un criterio per la atabilizzaazione della gallerie*. Gallerie e Grandi Opere Sotterranee, 29, 35-41.

Guan Zh., Jiang Y., Tanabasi Y., Huang H., 2007. *Reinforcement mechanics of passive bolts in conventional tunnelling.* International Journal of Rock Mechanics and Mining Science, 44, 4, 625-636.

Huang Z., Broch E., Lu M., 2002. *Cavern roof stability- mechanism of arching and stabilization by rockbolting*. Tunnelling and Underground Space Technology, 17, 3, 249-261.

Hoek E., Brown E.T., 1980. *Underground Excavations in Rock*. The Institution of Mining and Metallurgy, London.

Hoek E., Brown E.T., 1997. *Practical estimates of rock mass strength*. International Journal of Rock Mechanics and Mining Science, 34, 8, 1165-1187.

Indraratna B., Kaiser P.K., 1990a. *Design of grouted rock bolts based on the convergence control method*. International Journal of Rock Mechanics and Mining Science, 27, 4, 269-281.

Indraratna B., Kaiser P.K., 1990b. *Analytical model for the design of grouted rock bolts.* International Journal for Numerical and Analytical Methods in Geomechanics, 14, 4, 227-251.

Lee Y-K., Pietruszczak S., 2008. *A new numerical procedure for elasto-plastic analysis of a circular opening excavated in a strain-softening rock mass*. Tunnelling and Underground Space Technology, 23, 9, 588-599.

Li C., Stillborg B., 1999. *Analytical models for rock bolts*. International Journal of Rock Mechanics and Mining Science, 36, 8, 1013-1029.

Oreste P., 2003. *Analysis of structural interaction in tunnels using the convergence-confinement approach*. Tunnelling and Underground Space Technology, 18, 4, 347-363.

Oreste P., 2004. *Designing of radial bolting in tunnels*. Journal of Mining science, 40, 4, 384-394.

Oreste P., 2008. *Distinct analysis of fully grouted bolts around a circular tunnel considering the congruence of displacements between the bar and the rock.* International Journal of Rock Mechanics and Mining Science, 45, 7, 1052-1067.

Oreste P., 2009. *The convergence-confinement method: Roles and limits in modern geomechanical tunnel design.* American Journal of Applied Science, 6, 4, 757-771.

Osgoui R.R., Oreste P., 2007. *Convergence-control approach for rock tunnels reinforced by grouted bolts, using the homogenization concept*. Geotechnical and Geological Engineering, 25, 4, 431- 440.

Osgoui R.R., Oreste P., 2010. *Elasto-plastic analytical model for the design of grouted bolts in a Hoek-Brown medium*. International Journal for Numerical and Analytical Methods in Geomechanics, 34, 16, 1651-1686.

Park K-H., Tontavanich B., Lee J.G., 2008. *A simple procedure for ground response curve of circular tunnel in elastic--strain softening rock masses*. Tunnelling and Underground Space Technology, 23, 2, 151-159.

Peila D., Oreste P., 1995. *Axisymmetric analysis of ground reinforcing in tunneling design.* Computer and Geotechnics, 17, 2, 253-274.

Peila D., Oreste P., 1996. *Radial passive rockbolting in tunneling design with a new convergence-confinement model.* International Journal of Rock Mechanics and Mining Science, 33, 5, 443-454.

Ranjbarnia M., Fahimifar A., Oreste P., 2014a. *A simplified model to study the behaviour of pre-tensioned fully grouted bolts around tunnels and to analyse the more important influencing parameters*. Journal of Mining Science, 50, 3, 533-548.

Ranjbarnia M., Fahimifar A., Oreste P., 2014b. *Analysis of non-linear strain softening behaviour around tunnels*. Proceedings of the institution of civil engineers, 168, 1, 16-30.

Ranjbarnia M., Fahimifar A., Oreste P., 2015. *Practical Method for the Design of Pretensioned Fully-Grouted Rockbolts in Tunnels.* International Journal of geomechanics, 10.1061/ (ASCE) GM.1943-5622.0000464.

Ranjbarnia M., Oreste P., Fahimifar A., 2016. *Analytical-nimerical solution for stress distribution around tunnel reinforced by radial fully grouted rockbolts.* International Journal for Numerical and Analytical Methods in Geomechanics, 40, 13, 1844-1862.

Stille H., Holmberg M., Nord G., 1989. *Support of weak rock with grouted bolts and shotcrete*. International Journal of Rock Mechanics and Mining Science, 26, 1, 99-113.

Wang Sh., Yin X., Tang H., Ge X., 2010. *A new approach for analyzing circular tunnel in strain-softening rock masses*. International Journal of Rock Mechanics and Mining Science, 47, 1, 170-178.

Ward W.H., Coats D.J., Tedd P., 1976. *Performance of support systems in the Four Fathom Mudstone*. Proceedings of Tunnelling, London.

APPENDIX 1
Ground response curve calculation for reinforced rock mass

Input data

σ_c : un-axial compressive strength of intact rock pieces;
m, s : material constants for original rock mass;
E, v : Young's modulus and Poisson's ratio of original rock mass;
m_r, s_r : material constants for broken rock mass;
f, h : gradients of $-\varepsilon_3^p$ vs. $-\varepsilon_1^p$ lines;
α : constant defining strain at which residual strength is reached;
p_0 : in situ hydrostatic stress;
r_i : internal tunnel radius;
A_b : cross section area of each bolt;
E_s : Young's modulus of bolt;
C : bolt's spacing;
$T_{pre-ten}$: pre-tensioning force;

Preliminary Calculations

(1) $$M = \frac{1}{2}\left[\left(\frac{m}{4}\right)^2 + m\frac{p_0}{\sigma_c} + s\right]^{1/2} - \frac{m}{8}$$

(2) $$G = E/[2(1+\nu)]$$

(3) $$\varepsilon_{pre\text{–}ten} = T_{pre\text{–}ten}/(A_b E_s)$$

(4) $$r_{(1)} = r_e$$

(5) $$\varepsilon_{\theta(1)} = \varepsilon_{\theta(e)} = M\sigma_c/2G$$

(6) $$\varepsilon_{r(1)} = \varepsilon_{r(e)} = -M\sigma_c/2G$$

(7) $$\sigma_{r(1)} = \sigma_{re} = p_0 - M \cdot \sigma_c$$

(8) $$\sigma_{\theta(1)} = \sigma_{\theta(e)} = p_0 + M \cdot \sigma_c$$

(9) $$m_{(1)} = m$$

(10) $$s_{(1)} = s$$

(11) $$\omega_{(1)} = 0$$

(12) $$\lambda_1 = r_{(1)}/r_e = 1$$

Sequence of calculations for each ring by the first method

(1) $$d\varepsilon_\theta = 0.005\varepsilon_{\theta(1)}$$

(2) $$\varepsilon_{\theta(j)} = \varepsilon_{\theta(j-1)} + d\varepsilon_\theta$$

(3) If $\varepsilon_{\theta(j)} \le \alpha \cdot \varepsilon_{\theta(1)}$ then $\varepsilon_{r(j)} = \varepsilon_{r(j-1)} - hd\varepsilon_\theta$ otherwise $\varepsilon_{r(j)} = \varepsilon_{r(j-1)} - f \cdot d\varepsilon_\theta$

(4) $$\eta = \frac{2\varepsilon_{\theta(j-1)} - \varepsilon_{r(j-1)} - \varepsilon_{r(j)}}{2\varepsilon_{\theta(j)} - \varepsilon_{r(j-1)} - \varepsilon_{r(j)}}$$

(5) $$\lambda_{(j)} = \eta \cdot \lambda_{(j-1)}$$

(6) $$\lambda_{(j)} = r_{(j)}/r_e \qquad \lambda_{(j-1)} = r_{(j-1)}/r_e$$

(7) If $\varepsilon_{\theta(j)} \le \alpha \cdot \varepsilon_{\theta(1)}$ then $m_{(j)} = m + (m_r - m)\dfrac{\varepsilon_{\theta(j)} - \varepsilon_{\theta(e)}}{(\alpha - 1)\varepsilon_{\theta(e)}}$ otherwise $m_{(j)} = m_r$

(8) If $\varepsilon_{\theta(j)} \le \alpha \cdot \varepsilon_{\theta(1)}$ then $s_{(j)} = s + (s_r - s)\dfrac{\varepsilon_{\theta(j)} - \varepsilon_{\theta(e)}}{(\alpha - 1)\varepsilon_{\theta(e)}}$ otherwise $s_{(j)} = s_r$

(9) $$m_a = \frac{1}{2}\left(m_{(j-1)} + m_{(j)}\right)$$

(10) $$s_a = \frac{1}{2}\left(s_{(j-1)} + s_{(j)}\right)$$

(11) $$\chi_a = \frac{r_i}{\dfrac{r_{(j)} + r_{(j-1)}}{2}}$$

(12) $K_2 = \dfrac{m_a \sigma_c}{4}$

(13) $K = \dfrac{\lambda_{(j-1)} - \lambda_{(j)}}{\lambda_{(j)} + \lambda_{(j-1)}}$

(14) If $p_{pre-ten} \geq \beta \cdot p_0$, then go to step 15, otherwise go to step 21

(15) $\gamma_{pre-ten} = 2\varepsilon_{pre-ten}$

(16) $K_{pre-ten} = \dfrac{A_b E_s}{2C_0} \gamma_{pre-ten} \cdot \chi_a$

(17) $a^* = \dfrac{1}{4K^2}$

(18) $b^* = \dfrac{-K_{pre-ten}}{K} - \dfrac{\sigma_{r(j-1)}}{2K^2} - 2K_2$

(19) $c^* = \sigma_{r(j-1)} \left[\dfrac{\sigma_{r(j-1)}}{4K^2} + \dfrac{K_{pre-ten}}{K_2} - 2K_2 \right] + \left(K_{pre-ten} \right)^2 + 4\left(K_2 K_{pre-ten} \right) - s_a \sigma_c^2$

(20) Now, go to step 29

(21) $\gamma^* = \varepsilon_{r(j-1)} + \varepsilon_{r(j)}$

(22) $K_1^* = \dfrac{A_b E_s}{2C_0} \gamma^* \cdot \chi_a$

(23) If $\sigma_{r(j-1)} > \beta \cdot p_0$, then $\omega_{(j)} = 0$, otherwise $\omega_{(j)} = \omega_{(j-1)} + 1$

(24) $\bar{\gamma}^* = \bar{\varepsilon}_{r(j-1-\omega_{(j)})} + \bar{\varepsilon}_{r(j-\omega_{(j)})} \qquad r_i \leq r < \bar{r}_e$

$\gamma_e = \zeta \dfrac{M \sigma_C}{G} \qquad 0 < \zeta < 1 \qquad \bar{r}_e \leq r \leq r_e$

Note: the value of ζ has not great influence on ultimate solution.

(25) $\bar{K}_1^* = \dfrac{A_b E_s}{2C_0} \bar{\gamma}^* \chi_a \qquad r_i \leq r < \bar{r}_e$

$K_e = \dfrac{A_b E_s}{2C_0} \gamma_e \chi_a \qquad \bar{r}_e \leq r \leq r_e$

(26) $a^* = \dfrac{1}{4K^2}$

(27) $$b^* = \frac{\overline{K}_1^* - K_1^* - K_{pre-ten}}{K} - \frac{\sigma_{r(j-1)}}{2K^2} - 2K_2 \qquad r_i \le r < \overline{r}_e$$

$$b^* = \frac{K^{e(*)} - K_1^* + K_{pre-ten}}{K} - \frac{\sigma_{r(j-1)}}{2K^2} - 2K_2 \qquad \overline{r}_e \le r \le r_e$$

(28)
$$c^* = \sigma_{r(j-1)}\left[\frac{\sigma_{r(j-1)}}{4K^2} + \frac{K_1^* - \overline{K}_1^* + K_{pre-ten}}{K_2} - 2K_2\right] +$$
$$+\left(K_1^* - \overline{K}_1^* + K_{pre-ten}\right)^2 + 4\left(K_1^* K_2 - \overline{K}_1^* K_2 + K_2 K_{pre-ten}\right) - s_a\sigma_c^2$$
$$r_i \le r < \overline{r}_e$$

$$c^* = \sigma_{r(j-1)}\left[\frac{\sigma_{r(j-1)}}{4K^2} + \frac{K_1^* - K^{e(*)}}{K_2} - 2K_2\right] + \left(K_1^* - K^{e(*)} + K_{pre-ten}\right)^2$$
$$+4\left(K_1^* K_2 - K^{e(*)} K_2 + K_2 K_{pre-ten}\right) - s_a\sigma_c^2$$
$$\overline{r}_e \le r \le r_e$$

(29) $$\Delta = b^{*2} - 4a^* c^*$$

(30) $$\sigma_{r(j)} = \frac{-b^* - \sqrt{\Delta}}{2a^*}$$

(31) If $\sigma_{r(j)} > p_i$, then increment j by 1 and repeat the calculation sequence for next ring.

(32) If $\sigma_{r(j)} \approx p_i$, then $r_{(j)} = r_i$; $r_e = r_{(j)}/\lambda_{(j)}$.

Note: p_i should be gradually decreased to zero.

(32) If $\sigma_{r(j)} \approx \beta \cdot p_0$, then $\overline{r}_e = r_e$

(32) The radii of all the rings may now be calculated, using $r_{(j)} = \lambda_{(j)} \cdot r_e$

(32) The displacement values of rings may be determined from the previously computed values of $u_j = -\varepsilon_{\theta(j)} \cdot r_{(j)}$

Sequence of calculations for each ring by the second method

Steps (1) to (13) are repeated as for the first method.

(14) If $p_{pre-ten} \ge \beta \cdot p_0$, then go to step 15, otherwise go to step 19

(15) $$a^{**} = \frac{1}{4K^2}$$

(16) $$b^{**} = -\frac{\sigma_{r(j-1)}}{2K^2} - 2K_2$$

(17) $$c^{**} = \sigma_{r(j-1)}\left[\frac{\sigma_{r(j-1)}}{4K^2} - 2K_2\right] - s_a\sigma_c^2$$

(18) Now, go to step 27

(19) If $\sigma_{r(j-1)} > \beta \cdot p_0$ and then $\omega_{(j)} = 0$, other wise $\omega_{(j)} = \omega_{(j-1)} + 1$

(20) $$\gamma^{**} = d\varepsilon_{r(j)} = \varepsilon_{r(j)} - \varepsilon_{r(j-1)}$$

(21) $$K_1^{**} = \frac{A_b E_s r_i}{C_0\left(r_{(j-1)} - r_{(j)}\right)}\gamma^{**}$$

(22) $$\bar{\gamma}^{**} = d\bar{\varepsilon}_{r(j)} = \bar{\varepsilon}_{r(j-\omega_j)} - \bar{\varepsilon}_{r(j-1-\omega_j)} \qquad r_i \le r < \bar{r}_e$$

$$\gamma^{e(**)} = d\varepsilon^e_{r(j)} = \varepsilon^e_{r(j)} - \varepsilon^e_{r(j-1)} \qquad \bar{r}_e \le r \le r_e$$

(23) $$\bar{K}_1^{**} = \frac{A_b E_s r_i}{C_0\left(r_{(j-1)} - r_{(j)}\right)}\bar{\gamma}^{**} \qquad r_i \le r < \bar{r}_e$$

$$K_1^{e(**)} = \frac{A_b E_s r_i}{C_0\left(r_{(j-1)} - r_{(j)}\right)}\gamma^{e(**)} \qquad \bar{r}_e \le r \le r_e$$

(24) $$a^{**} = \frac{1}{4K^2}$$

(25) $$b^{**} = -\frac{K_1^{**} - \bar{K}_1^{**}}{K} - \frac{\sigma_{r(j-1)}}{2K^2} - 2K_2 \qquad r_i \le r < \bar{r}_e$$

$$b^{**} = -\frac{K_1^{**} - K_1^{e(**)}}{K} - \frac{\sigma_{r(j-1)}}{2K^2} - 2K_2 \qquad \bar{r}_e \le r \le r_e$$

(26) $$c^{**} = \sigma_{r(j-1)}\left[\frac{\sigma_{r(j-1)}}{4K^2} + \frac{K_1^{**} - \bar{K}_1^{**}}{K} - 2K_2\right] + \left(K_1^{**} - \bar{K}_1^{**}\right)^2 - s_a\sigma_c^2 \qquad r_i \le r < \bar{r}_e$$

$$c^{**} = \sigma_{r(j-1)}\left[\frac{\sigma_{r(j-1)}}{4K^2} + \frac{K_1^{**} - K_1^{e(**)}}{K} - 2K_2\right] + \left(K_1^{**} - K_1^{e(**)}\right)^2 - s_a\sigma_c^2 \qquad \bar{r}_e \le r \le r_e$$

(27) $$\Delta = b^{**2} - 4a^{**}c^{**}$$

(28) $$\sigma_{r(j)} = \frac{-b^{**} - \sqrt{\Delta}}{2a^{**}}$$

(29) If $\sigma_{r(j)} > p_i$, then increment j by 1 and repeat the calculation sequence for next ring.

(30) If $\sigma_{r(j)} \approx p_i$, then $r_{(j)} = r_i$; $r_e = r_{(j)}/\lambda_{(j)}$.

Note: p_i should not be decreased from $p_{pre\text{–}ten}$.

(31) If $\sigma_{r(j)} \approx \beta \cdot p_0$, then $\bar{r}_e = r_e$

(32) The radii of all the rings may now be calculated, using $r_{(j)} = \lambda_{(j)} \cdot r_e$

(33) The displacement values of rings may be determined from the previously computed values of $u_j = -\varepsilon_{\theta(j)} \cdot r_{(j)}$